

Correspondence: Amer M. Zeidan, Section of Hematology, Department of Internal Medicine, Yale University, 333 Cedar St, PO Box 208028, New Haven, CT 06520-8028; e-mail: amer.zeidan@yale.edu.

## Footnote

Presented in oral form at the 59th annual meeting of the American Society of Hematology, Atlanta, GA, 9-12 December 2017.

## REFERENCES

- Fenaux P, Mufti GJ, Hellström-Lindberg E, et al. Azacitidine prolongs overall survival compared with conventional care regimens in elderly patients with low bone marrow blast count acute myeloid leukemia. *J Clin Oncol*. 2010;28(4):562-569.
- Steensma DP. Myelodysplastic syndromes: diagnosis and treatment. *Mayo Clin Proc*. 2015;90(7):969-983.
- Platzbecker U. Who benefits from allogeneic transplantation for myelodysplastic syndromes? New insights. *Hematology Am Soc Hematol Educ Program*. 2013;2013:522-528.
- Zeidan AM, Linhares Y, Gore SD. Current therapy of myelodysplastic syndromes. *Blood Rev*. 2013;27(5):243-259.
- Ma X, Does M, Raza A, Mayne ST. Myelodysplastic syndromes: incidence and survival in the United States. *Cancer*. 2007;109(8):1536-1542.
- Craig BM, Rollison DE, List AF, Cogle CR. Underreporting of myeloid malignancies by United States cancer registries. *Cancer Epidemiol Biomarkers Prev*. 2012;21(3):474-481.
- Fritz A, ed. International classification of diseases for oncology. 3rd ed. Lyon, France: International Agency for Research on Cancer, World Health Organization; 2000.
- Elixhauser A, Steiner C, Harris DR, Coffey RM. Comorbidity measures for use with administrative data. *Med Care*. 1998;36(1):8-27.
- Zeidan AM, Sekeres MA, Garcia-Manero G, et al; MDS Clinical Research Consortium. Comparison of risk stratification tools in predicting outcomes of patients with higher-risk myelodysplastic syndromes treated with azanucleosides. *Leukemia*. 2016;30(3):649-657.
- Bernal T, Martínez-Cambor P, Sánchez-García J, et al; Spanish Society of Hematology. Effectiveness of azacitidine in unselected high-risk myelodysplastic syndromes: results from the Spanish registry. *Leukemia*. 2015;29(9):1875-1881.
- Itzykson R, Thépot S, Quesnel B, et al; Groupe Francophone des Myelodysplasies (GFM). Prognostic factors for response and overall survival in 282 patients with higher-risk myelodysplastic syndromes treated with azacitidine. *Blood*. 2011;117(2):403-411.
- Zeidan AM, Davidoff AJ, Long JB, et al. Comparative clinical effectiveness of azacitidine versus decitabine in older patients with myelodysplastic syndromes. *Br J Haematol*. 2016;175(5):829-840.
- Zeidan AM, Wang R, Gross CP, et al. Modest improvement in survival of patients with refractory anemia with excess blasts in the hypomethylating agents era in the United States. *Leuk Lymphoma*. 2017;58(4):982-985.
- Zeidan AM, Stahl M, Sekeres MA, Steensma DP, Komrokji RS, Gore SD. A call for action: Increasing enrollment of untreated patients with higher-risk myelodysplastic syndromes in first-line clinical trials. *Cancer*. 2017;123(19):3662-3672.

DOI 10.1182/blood-2017-10-811729

© 2018 by The American Society of Hematology

## TO THE EDITOR:

# Five percent of healthy newborns have an *ETV6-RUNX1* fusion as revealed by DNA-based GIPFEL screening

Daniel Schäfer,<sup>1</sup> Marianne Olsen,<sup>2</sup> David Lähnemann,<sup>1,3</sup> Martin Stanulla,<sup>4</sup> Robert Slany,<sup>5</sup> Kjeld Schmiegelow,<sup>2,6</sup> Arndt Borkhardt,<sup>1</sup> and Ute Fischer<sup>1</sup>

<sup>1</sup>Department of Pediatric Oncology, Hematology, and Clinical Immunology, University Children's Hospital, Medical Faculty, Heinrich Heine University, Düsseldorf, Germany; <sup>2</sup>Department of Pediatrics and Adolescent Medicine, The Juliane Marie Centre, The University Hospital Rigshospitalet, Copenhagen, Denmark; <sup>3</sup>Computational Biology of Infection Research, Helmholtz Centre for Infection Research, Braunschweig, Germany; <sup>4</sup>Department of Pediatric Hematology and Oncology, Hannover Medical School, Hannover, Germany; <sup>5</sup>Department of Genetics, Friedrich Alexander University, Erlangen-Nuremberg, Germany; and <sup>6</sup>Institute of Clinical Medicine, Faculty of Medicine, University of Copenhagen, Copenhagen, Denmark

Pediatric acute lymphoblastic leukemia (ALL) is characterized by recurrent preleukemic chromosomal translocations that emerge frequently in utero.<sup>1</sup> The most common translocation t(12;21) occurs in 25% of B-cell precursor ALL and results in the formation of the chimeric transcription factor *ETV6-RUNX1*. Secondary oncogenic hits acquired postnatally are necessary to develop overt leukemia.<sup>2,3</sup> Therefore, the number of newborns harboring a preleukemic translocation is expected to equal or exceed the incidence of the corresponding leukemia.

In 2002, Mel Greaves' group analyzed the frequency of *ETV6-RUNX1* translocations in human newborns by independent reverse transcriptase (RT)-polymerase chain reaction (PCR) and quantitative PCR (qPCR) screens confirmed by multicolor fluorescence in situ hybridization. They observed that ≈1% of cord bloods from newborns (n = 6 of 567) contained *ETV6-RUNX1*<sup>+</sup> cells.<sup>4</sup> The translocation seemed to occur frequently during

normal fetal development and to be 100-fold more common than the corresponding leukemia (1 in 10 000 children). This indicated a very low oncogenic potential of the *ETV6-RUNX1* transcription factor and suggested that the usefulness of preventive screenings of *ETV6-RUNX1*-carrying newborns is limited because 99% would never develop the disease.

Since this initial investigation, several studies have carefully analyzed the incidence of the translocation in newborns, children, and adults using fresh or frozen cord blood or peripheral blood (summarized in supplemental Table 1, available on the *Blood* Web site).<sup>4-14</sup> Remarkably, the suggested incidence ranged from 0.01% (equaling the corresponding leukemia rate)<sup>7-9</sup> to ≈8% (exceeding it by a factor of 800).<sup>5</sup> Because the investigated cohorts and specimens were similar, the variation was assumed to have technical explanations. Also, the frequency of preleukemic cells in healthy blood or cord blood was controversially discussed, ranging from <10<sup>-5</sup> to 10<sup>-3</sup>.

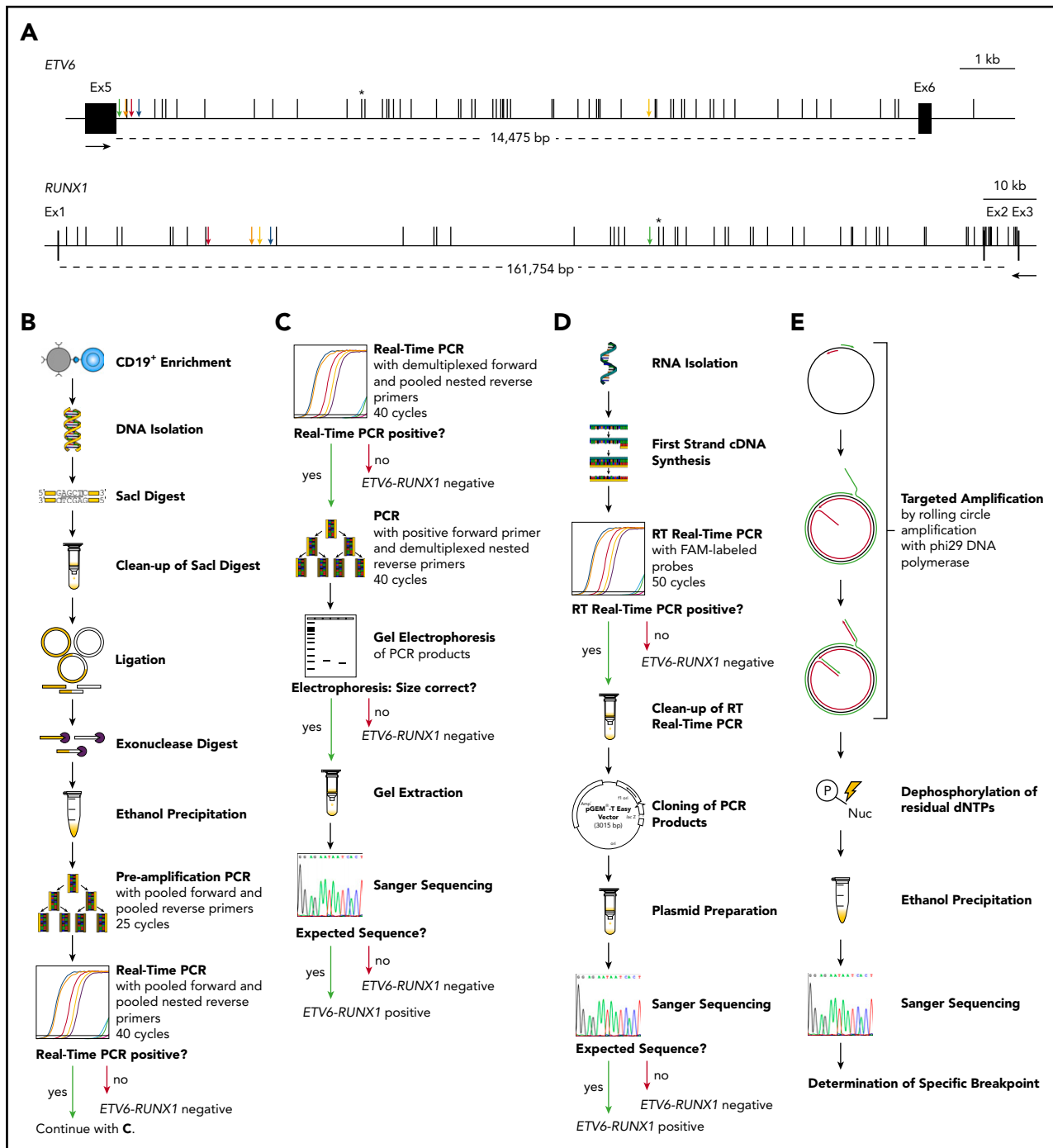


**Figure 1. The incidence of *ETV6-RUNX1* fusions in healthy newborns can be determined by DNA-based GIPFEL screening.** (A) Only DNA- and not RNA-based *ETV6-RUNX1* detection provides individual-specific breakpoints. The breakpoint cluster regions (BCRs; horizontal lines, exact regions are marked by dotted lines, sizes are given in base pairs) of *ETV6* (top panel, intron 5) and *RUNX1* (bottom panel, intron 1 and 2) are presented. Black boxes indicate exons and vertical black lines on top of the BCRs indicate reported patient-specific breakpoints.<sup>21-25</sup> Asterisks mark the breakpoint present in the REH cell line. The breakpoints identified in the present study are indicated by orange (N424), blue (N726), red (N817), green (N823), and yellow (N890) arrows. Black arrows represent primers that are usually used for *ETV6-RUNX1* screening by RT-PCR. They generate 1 of 2 PCR products for every possible breakpoint within the BCRs: exon 5 of *ETV6* fused to either exon 2 or exon 3 of *RUNX1*. Only DNA-based techniques can differentiate between breakpoints that are specific for each individual patient and localized in intronic regions. (B-E) The workflow of cord blood screening using a modified GIPFEL technique<sup>15</sup> is presented. (B) CD19<sup>+</sup> B cells were enriched from newborn cord blood. DNA was isolated, fragmented using *SacI*, and purified. The DNA was ligated to achieve circularization and residual linear DNA was digested. DNA circles were purified and PCR (preamplification) and real-time PCR were used to detect the ligation joints produced by circularization. The protocol was carried out with each sample. (C) Optional continuation protocol that was carried out if the real-time PCR in panel B generated a putative positive result. Then a new real-time PCR was carried out with demultiplexed forward primers. If 1 of the forward primers produced a positive result, the PCR was repeated with this forward primer and demultiplexed reverse primers. The products were then analyzed on an agarose gel and Sanger sequenced. In case of negative results, no further validation steps were done. (D) Workflow of the transcriptional validation. RNA was reverse transcribed and subjected to real-time PCR. In case of a putative positive result, the PCR product was purified, cloned, and subjected to Sanger sequencing. (E) Further development of the original GIPFEL technique allowed the identification of patient-specific breakpoints with base-pair resolution. To this end, circularized DNA was amplified using specific primers that hybridized to the known ligation joint region and faced toward the unknown breakpoint. Amplification was carried out with *Phi29* DNA polymerase, leading to linear products. With *Phi29*, amplification occurs at a constant temperature and new primers can constantly bind to the original and the amplified DNA, leading to further amplification. The amplified DNA was subsequently purified and Sanger sequenced. cDNA, complementary DNA; dNTP, deoxynucleotide triphosphate; Ex, exon; FAM, fluorescein amidite; Nuc, deoxynucleoside diphosphate; P, phosphate.

**Table 1. Fifty of 1000 cord bloods from healthy newborns were *ETV6-RUNX1* translocation-positive in GIPFEL screening**

Healthy newborn	Multiplexed primer group	Forward primer	<i>RUNX1</i> intron	Reverse primer	<i>ETV6</i> intron	Estimated frequency
N005	3	RUNX1-S6f	1	ETV6-S1r-n	5	$1 \times 10^{-4}$
N059	4	RUNX1-S13f	1	ETV6-S2r-n	5	$6 \times 10^{-3}$
N099	3	RUNX1-S2f	2	ETV6-S2r-n	5	$2 \times 10^{-4}$
N260	2	RUNX1-S14f	1	ETV6-S2r-n	5	$1.5 \times 10^{-4}$
N285	2	RUNX1-S11f	1	ETV6-S1r-n	5	$8 \times 10^{-4}$
N286	3	RUNX1-S8f	1	ETV6-S1r-n	5	$1 \times 10^{-4}$
N382	2	RUNX1-S11f	1	ETV6-S3r-n	5/6	$1 \times 10^{-3}$
N424*	1	RUNX1-S23f	1	ETV6-S1r-n	5	$5 \times 10^{-4}$
N439	1	RUNX1-S23f	1	ETV6-S1r-n	5	$4 \times 10^{-4}$
N440	3	RUNX1-S18f	1	ETV6-S2r-n	5	$1 \times 10^{-3}$
N441	1	RUNX1-S22f	1	ETV6-S2r-n	5	$1 \times 10^{-4}$
N447	1	RUNX1-S28f	1	ETV6-S3r-n	5/6	$2 \times 10^{-3}$
N463	2	RUNX1-S10f	1	ETV6-S2r-n	5	$3 \times 10^{-4}$
N472	4	RUNX1-S21f	1	ETV6-S3r-n	5/6	$1 \times 10^{-4}$
N479	4	RUNX1-S13f	1	ETV6-S2r-n	5	$1 \times 10^{-3}$
N493	3	RUNX1-S18f	1	ETV6-S2r-n	5	$1 \times 10^{-2}$
N496	4	RUNX1-S5f	1	ETV6-S1r-n	5	$1.5 \times 10^{-3}$
<b>N505</b>	<b>2</b>	<b>RUNX1-S11f</b>	<b>1</b>	<b>ETV6-S3r-n</b>	<b>5/6</b>	<b><math>4 \times 10^{-3}</math></b>
<b>N505</b>	<b>4</b>	<b>RUNX1-S13f</b>	<b>1</b>	<b>ETV6-S1r-n</b>	<b>5</b>	<b><math>7 \times 10^{-4}</math></b>
N506	1	RUNX1-S28f	1	ETV6-S1r-n	5	$5 \times 10^{-3}$
N521	2	RUNX1-S4f	1	ETV6-S2r-n	5	$4 \times 10^{-2}$
N522	2	RUNX1-S10f	1	ETV6-S2r-n	5	$1 \times 10^{-2}$
N527	4	RUNX1-S21f	1	ETV6-S1r-n	5	$4 \times 10^{-3}$
<b>N531</b>	<b>3</b>	<b>RUNX1-S29f</b>	<b>1</b>	<b>ETV6-S2r-n</b>	<b>5</b>	<b><math>5 \times 10^{-3}</math></b>
<b>N531</b>	<b>4</b>	<b>RUNX1-S13f</b>	<b>1</b>	<b>ETV6-S2r-n</b>	<b>5</b>	<b><math>1.5 \times 10^{-3}</math></b>
N548	4	RUNX1-S21f	1	ETV6-S2r-n	5	$9 \times 10^{-5}$
N563	2	RUNX1-S11f	1	ETV6-S2r-n	5	$8 \times 10^{-4}$
N578	2	RUNX1-S24f	1	ETV6-S3r-n	5/6	$8 \times 10^{-5}$
N590	1	RUNX1-S26f	1	ETV6-S1r-n	5	$4 \times 10^{-4}$
N599	2	RUNX1-S10f	1	ETV6-S3r-n	5/6	$5 \times 10^{-3}$
N619	4	RUNX1-S5f	1	ETV6-S3r-n	5/6	$6 \times 10^{-3}$
N622	1	RUNX1-S26f	1	ETV6-S2r-n	5	$3 \times 10^{-4}$

Frequencies refer to B-cell population. Results for 2 newborns with concurrent fusions appear in bold.

\*In these cases, the translocation was confirmed by Sanger sequencing of the breakpoint.

**Table 1. (continued)**

Healthy newborn	Multiplexed primer group	Forward primer	<i>RUNX1</i> intron	Reverse primer	<i>ETV6</i> intron	Estimated frequency
N630	1	RUNX1-S12f	1	ETV6-S2r-n	5	$1 \times 10^{-2}$
N651	2	RUNX1-S4f	1	ETV6-S2r-n	5	$1 \times 10^{-4}$
N670	1	RUNX1-S12f	1	ETV6-S3r-n	5/6	$1 \times 10^{-2}$
N673	3	RUNX1-S8f	1	ETV6-S2r-n	5	$1 \times 10^{-2}$
N674	1	RUNX1-S28f	1	ETV6-S3r-n	5/6	$9 \times 10^{-3}$
N726*	1	RUNX1-S22f	1	ETV6-S1r-n	5	$4 \times 10^{-5}$
N729	1	RUNX1-S23f	1	ETV6-S3r-n	5/6	$5 \times 10^{-5}$
N731	2	RUNX1-S4f	1	ETV6-S3r-n	5/6	$1.5 \times 10^{-5}$
N732	2	RUNX1-S10f	1	ETV6-S2r-n	5	$1 \times 10^{-4}$
N770	4	RUNX1-S13f	1	ETV6-S3r-n	5/6	$4 \times 10^{-4}$
N775	2	RUNX1-S14f	1	ETV6-S2r-n	5	$1 \times 10^{-3}$
N784	1	RUNX1-S28f	1	ETV6-S2r-n	5	$3 \times 10^{-4}$
N791	3	RUNX1-S6f	1	ETV6-S2r-n	5	$1 \times 10^{-4}$
N795	2	RUNX1-S24f	1	ETV6-S3r-n	5/6	$1 \times 10^{-4}$
N817*	4	RUNX1-S25f	1	ETV6-S1r-n	5	$2 \times 10^{-3}$
N823*	4	RUNX1-S13f	1	ETV6-S1r-n	5	$1 \times 10^{-3}$
N890*	1	RUNX1-S23f	1	ETV6-S3r-n	5/6	$1 \times 10^{-3}$
N908	1	RUNX1-S15f	1	ETV6-S3r-n	5/6	$6 \times 10^{-4}$
N912	2	RUNX1-S24f	1	ETV6-S2r-n	5	$3 \times 10^{-3}$
N926	4	RUNX1-S5f	1	ETV6-S3r-n	5/6	$3 \times 10^{-4}$

Frequencies refer to B-cell population. Results for 2 newborns with concurrent fusions appear in bold.

\*In these cases, the translocation was confirmed by Sanger sequencing of the breakpoint.

All of the previous studies used RNA and RT-PCR for prevalence determination. A drawback of RT-PCR is the possible generation of false-positive results caused by contamination. These false-positive results cannot be distinguished from real ones, as for a given translocation the identical amplification products are created in different samples.<sup>9</sup> In addition, low levels of positivity can be due to RNA instability, different processing of RNA, detection methods, and, possibly, low expression of *ETV6-RUNX1* transcripts in cord blood.

To analyze the frequency of *ETV6-RUNX1*<sup>+</sup> preleukemic cells in newborns, we therefore developed a DNA-based method termed genomic inverse PCR for exploration of ligated breakpoints (GIPFEL)<sup>15</sup> because DNA, in contrast to RNA, is very stable. By DNA-based approaches, patient-specific amplification products of the translocation site that differ from one another in size and sequence are obtained and contaminations can be easily identified (Figure 1A). The advantages of DNA-based screening methods have led to an increased use in clinical applications

(eg, DNA-based monitoring of minimal residual disease in *BCR-ABL*<sup>+</sup> leukemia<sup>16</sup>).

GIPFEL is capable of detecting gene fusions without prior knowledge of the exact breakpoint by exploiting the presence of genomic fragments that join material from known regions of 2 different chromosomes. These fragments can be digested and circularized by ligation, creating a junction across the restriction site whose sequence can be predicted from published genome data and used for the design of real-time PCRs.

For *ETV6-RUNX1* fusion detection, genomic DNA is digested by *SacI* and circularized by intramolecular ligation (Figure 1B-E; supplemental Methods; supplemental Figure 1). A multiplexed, semi-nested real-time PCR is performed to quantify translocation-specific ligation products. Demultiplexed qPCR, gel electrophoresis, and sequencing are used for validation of the ligation product and to narrow down the breakpoint

region. GIPFEL can detect 1 translocation-carrying cell within 10 000 normal cells (sensitivity  $\approx 10^{-4}$ ) and is highly specific. The likelihood that GIPFEL produces false-positive signals is extremely low ( $\ll 10^{-10}$ ; supplemental Figure 2) and has so far never been observed (eg, >180 negative controls for *ETV6-RUNX1*).

Here, we applied GIPFEL to a retrospective screening of 1000 newborns. The study was approved by the Danish Data Protection Agency and the Danish Scientific Ethics Committee. Written informed consent was obtained. After B-cell enrichment, genomic DNA was prepared from cryopreserved cord bloods and GIPFEL was carried out. In 50 of 1000 samples, sequencing of the ligation joints validated a signal compatible with *ETV6-RUNX1* translocation (Table 1; supplemental Figures 3 and 4). These data suggest that  $\approx 5\%$  of newborns harbor the *ETV6-RUNX1* fusion at levels detectable by GIPFEL.

GIPFEL screening also revealed 2 newborns (N505, N531) whose cord blood harbored 2 different *ETV6-RUNX1* fusions each (Table 1; supplemental Figure 5). The estimated frequencies of the 2 fusions differed from one another (N505:  $4 \times 10^{-3}$  and  $7 \times 10^{-4}$ , N531:  $5 \times 10^{-3}$  and  $1.5 \times 10^{-3}$ ), indicating 2 coexisting or overlapping clones.

To validate our screening results, we tested fusion transcript expression in GIPFEL<sup>+</sup> and GIPFEL<sup>-</sup> cord bloods by qPCR (Figure 1D; supplemental Figure 6; supplemental Table 2). Due to limited sample availability, we could only investigate 2 positive (N005 and N260) and 50 negative cord bloods. In the REH cell line, *ETV6-RUNX1* expression was roughly in the same range as the *ABL1* control gene. In GIPFEL<sup>+</sup> cord blood samples, expression of *ETV6-RUNX1* was detected at a lower level ( $10^{-4}$ ) in accord with the lower number of translocation-carrying cells ( $10^{-4}$ ) compared with the cell line. We confirmed the fusions on the RNA level by Sanger sequencing. None of the GIPFEL<sup>-</sup> cord bloods showed transcription of *ETV6-RUNX1*. In addition, 9 translocation-negative cell lines were both GIPFEL<sup>-</sup> and qPCR<sup>-</sup> (supplemental Table 3).

To finally confirm positive GIPFEL results, we sequenced individual-specific breakpoints with base-pair resolution on the DNA level using targeted amplification of translocation-carrying circles and Sanger sequencing (Figure 1E). Due to limited sample availability, *ETV6-RUNX1* breakpoints of 5 cord bloods (N424, N726, N817, N832, N890) have been identified so far (Figure 1A; supplemental Figure 7). The breakpoints were specific for each proband and never reported before.

Because of anonymized sample processing, no tracking of leukemia cases within the analyzed cohort could be carried out. However, the determined frequencies of *ETV6-RUNX1* translocations ( $\approx 5\%$  GIPFEL screen or  $\approx 0.5\%$  if taking into account only GIPFEL screen results validated by breakpoint sequencing) are both far above the leukemia frequency of  $\approx 0.01\%$ . The incidence of *ETV6-RUNX1* fusions may even exceed  $\approx 5\%$  because complex rearrangements, rearrangements outside of the known breakpoint regions, and not-yet-expanded cell clones ( $< 10^{-4}$ ) evade detection by GIPFEL.<sup>15</sup> Thus, translocation-carrying clones (and potentially >1) are likely present in a high number of healthy

individuals who will never develop leukemia. Similarly, other leukemia- or lymphoma-associated translocations have been detected in peripheral blood of healthy individuals (reviewed in Janz et al<sup>17</sup>). Illegitimate genetic recombination seems to occur frequently in hematopoietic precursors. For preleukemic clones to arise, the fusion has to occur in an early precursor with self-renewal capacity and must produce a functional oncoprotein that promotes clonal expansion.

In the case of *ETV6-RUNX1*, the leukemia-inducing potential of the fusion seems to be very low. This is in accordance with (1) the low concordance rate of  $\approx 10\%$  in identical twins,<sup>18</sup> (2) the long postnatal latency phase ( $\approx 2$ -14 years),<sup>2</sup> (3) the presence of recurrent secondary leukemia inducing genetic lesions (*ETV6* deletions in 70%, extra copies of *RUNX1* in 23%, or extra der(21)t(12;21) in 10% of cases),<sup>19</sup> and (4) evidence from transgenic animal studies.<sup>20</sup>

These results strengthen the importance of environmentally or spontaneously caused secondary hits in *ETV6-RUNX1*<sup>+</sup> ALL. Future studies correlating GIPFEL screens with genetic and epidemiological data will provide closer insight into the pathogenesis of *ETV6-RUNX1*<sup>+</sup> leukemia.

## Acknowledgments

The authors thank Sabine Hornhardt (Federal Office for Radiation Protection, Oberschleissheim, Germany) for advice and support. The authors thank Mel Greaves and Tony Ford (The Institute of Cancer Research, London, United Kingdom) and Jan Trka (Childhood Leukaemia Investigation Prague, Prague, Czech Republic) for valuable comments. The authors thank their colleague Cyrill Schipp for valuable support and Daniel Scholtysik and Bianca Killing for excellent technical assistance.

This work was supported by the German Federal Office for Radiation Protection (grant 36 14 S 30034), by an intramural grant (2016-70) of the Research Commission of the Medical Faculty of Heinrich Heine University Düsseldorf, by the Katharina-Hardt-Stiftung, by the Danish Cancer Society, and by the Danish Childhood Cancer Foundation.

## Authorship

Contribution: D.S. performed laboratory work, designed research, analyzed data, and wrote the paper; D.L. designed research and critically reviewed the paper; M.S. provided clinical samples and analyzed clinical data; R.S. designed research; M.O. recruited the probands, analyzed clinical data, and designed and performed laboratory work; K.S. designed and supervised research; A.B. designed research and wrote the paper; U.F. designed research, analyzed data, and wrote the paper; and U.F. and A.B. were the principal investigators and take primary responsibility for the paper.

Conflict-of-interest disclosure: The authors declare no competing financial interests.

Correspondence: Ute Fischer, Department of Pediatric Oncology, Hematology, and Clinical Immunology, Center for Child and Adolescent Health, Heinrich Heine University, Moorenstr 5, 40225 Düsseldorf, Germany; e-mail: ute.fischer@med.uni-duesseldorf.de.

## Footnote

The online version of this article contains a data supplement.

## REFERENCES

- Mullighan CG. Molecular genetics of B-precursor acute lymphoblastic leukemia. *J Clin Invest*. 2012;122(10):3407-3415.
- Wiemels JL, Ford AM, Van Wering ER, Postma A, Greaves M. Protracted and variable latency of acute lymphoblastic leukemia after TEL-AML1 gene fusion in utero. *Blood*. 1999;94(3):1057-1062.
- Papaemmanuil E, Rapado I, Li Y, et al. RAG-mediated recombination is the predominant driver of oncogenic rearrangement in ETV6-RUNX1 acute lymphoblastic leukemia. *Nat Genet*. 2014;46(2):116-125.
- Mori H, Colman SM, Xiao Z, et al. Chromosome translocations and covert leukemic clones are generated during normal fetal development. *Proc Natl Acad Sci USA*. 2002;99(12):8242-8247.
- Eguchi-Ishimae M, Eguchi M, Ishii E, et al. Breakage and fusion of the TEL (ETV6) gene in immature B lymphocytes induced by apoptogenic signals. *Blood*. 2001;97(3):737-743.
- Olsen M, Madsen HO, Hjalgrim H, Gregers J, Rostgaard K, Schmiegelow K. Preleukemic TEL-AML1-positive clones at cell level of 10<sup>-3</sup> to 10<sup>-4</sup> do not persist into adulthood. *J Pediatr Hematol Oncol*. 2006;28(11):734-740.
- Lausten-Thomsen U, Hjalgrim H, Marquart H, Lutterodt M, Petersen BL, Schmiegelow K. ETV6-RUNX1 transcript is not frequent in early human haematopoiesis. *Eur J Haematol*. 2008;81(2):161-162.
- Lausten-Thomsen U, Madsen HO, Vestergaard TR, Hjalgrim H, Lando A, Schmiegelow K. Increased risk of ALL among premature infants is not explained by increased prevalence of pre-leukemic cell clones. *Blood Cells Mol Dis*. 2010;44(3):188-190.
- Lausten-Thomsen U, Madsen HO, Vestergaard TR, Hjalgrim H, Nersting J, Schmiegelow K. Prevalence of t(12;21)[ETV6-RUNX1]-positive cells in healthy neonates. *Blood*. 2011;117(1):186-189.
- Zuna J, Madzo J, Krejci O, et al. ETV6/RUNX1 (TEL/AML1) is a frequent prenatal first hit in childhood leukemia. *Blood*. 2011;117(1):368-369; author reply 370-371.
- Olsen M, Hjalgrim H, Melbye M, Madsen HO, Schmiegelow K. RT-PCR screening for ETV6-RUNX1-positive clones in cord blood from newborns in the Danish National Birth Cohort. *J Pediatr Hematol Oncol*. 2012;34(4):301-303.
- Škorvaga M, Nikitina E, Kubeš M, et al. Incidence of common preleukemic gene fusions in umbilical cord blood in Slovak population. *PLoS One*. 2014;9(3):e91116.
- Ornelles DA, Gooding LR, Garnett-Benson C. Neonatal infection with species C adenoviruses confirmed in viable cord blood lymphocytes. *PLoS One*. 2015;10(3):e0119256.
- Kosik P, Skorvaga M, Durdik M, et al. Low numbers of pre-leukemic fusion genes are frequently present in umbilical cord blood without affecting DNA damage response. *Oncotarget*. 2017;8(22):35824-35834.
- Fueller E, Schaefer D, Fischer U, et al. Genomic inverse PCR for exploration of ligated breakpoints (GIPFEL), a new method to detect translocations in leukemia. *PLoS One*. 2014;9(8):e104419.
- Hovorkova L, Zaliova M, Venn NC, et al. Monitoring of childhood ALL using BCR-ABL1 genomic breakpoints identifies a subgroup with CML-like biology. *Blood*. 2017;129(20):2771-2781.
- Janz S, Potter M, Rabkin CS. Lymphoma- and leukemia-associated chromosomal translocations in healthy individuals. *Genes Chromosomes Cancer*. 2003;36(3):211-223.
- Greaves MF, Maia AT, Wiemels JL, Ford AM. Leukemia in twins: lessons in natural history. *Blood*. 2003;102(7):2321-2333.
- Sun C, Chang L, Zhu X. Pathogenesis of ETV6/RUNX1-positive childhood acute lymphoblastic leukemia and mechanisms underlying its relapse. *Oncotarget*. 2017;8(21):35445-35459.
- Hauer J, Borkhardt A, Sánchez-García I, Cobaleda C. Genetically engineered mouse models of human B-cell precursor leukemias. *Cell Cycle*. 2014;13(18):2836-2846.
- Wiemels JL, Greaves M. Structure and possible mechanisms of TEL-AML1 gene fusions in childhood acute lymphoblastic leukemia. *Cancer Res*. 1999;59(16):4075-4082.
- Wiemels JL, Alexander FE, Cazzaniga G, Biondi A, Mayer SP, Greaves M. Microclustering of TEL-AML1 translocation breakpoints in childhood acute lymphoblastic leukemia. *Genes Chromosomes Cancer*. 2000;29(3):219-228.
- Andersen MT, Nordentoft I, Hjalgrim LL, et al. Characterization of t(12;21) breakpoint junctions in acute lymphoblastic leukemia. *Leukemia*. 2001;15(5):858-859.
- Rodríguez-Hernández G, Hauer J, Martín-Lorenzo A, et al. Infection exposure promotes ETV6-RUNX1 precursor B-cell leukemia via impaired H3K4 demethylases. *Cancer Res*. 2017;77(16):4365-4377.
- Jin Y, Wang X, Hu S, Tang J, Li B, Chai Y. Determination of ETV6-RUNX1 genomic breakpoint by next-generation sequencing. *Cancer Med*. 2016;5(2):337-351.

DOI 10.1182/blood-2017-09-808402

© 2018 by The American Society of Hematology

## TO THE EDITOR:

# Loss of RKIP is a frequent event in myeloid sarcoma and promotes leukemic tissue infiltration

Veronica Caraffini,<sup>1</sup> Bianca Perfler,<sup>1</sup> Johannes Lorenz Berg,<sup>1</sup> Barbara Uhl,<sup>1</sup> Silvia Schauer,<sup>2</sup> Karl Kashofer,<sup>2</sup> Nassim Ghaffari-Tabrizi-Wizsy,<sup>3</sup> Herbert Strobl,<sup>3</sup> Albert Wölfler,<sup>1</sup> Gerald Hoefler,<sup>2</sup> Heinz Sill,<sup>1</sup> and Armin Zebisch<sup>1</sup>

<sup>1</sup>Division of Hematology, <sup>2</sup>Institute of Pathology, and <sup>3</sup>Institute of Pathophysiology and Immunology, Medical University of Graz, Graz, Austria

Myeloid sarcoma (MS) is a subtype of acute myeloid leukemia (AML), in which leukemic cells invade extramedullary tissues and form solid tumors.<sup>1-3</sup> MS may manifest as an isolated event or with concomitant involvement of leukemic bone marrow (BM), the latter affecting up to 20% to 30% of all AML cases.<sup>2,4-8</sup> Clinical data about the prognostic relevance of MS are still conflicting, mainly because of variable clearing of extramedullary leukemic blasts by conventional chemotherapy.<sup>2,7,9</sup> Hence, knowledge of the pathogenetic mechanisms, which endow leukemic blasts

with an invasive potential and thereby cause the formation of MS, will help to improve therapeutic regimens for MS patients. RAF kinase inhibitor protein (RKIP) is a negative regulator of RAS-MAPK/ERK signaling.<sup>10-12</sup> A somatic loss of RKIP has recently been described as a frequent event in AML. It has been shown to be associated with monocytic AML phenotypes and proven to be of functional relevance for leukemogenesis.<sup>13-15</sup> It is interesting to note that RKIP loss has also been observed in a variety of solid cancers and has been described as a bona fide